[redacted]

[redacted]

Copy No. 113
RM No. L8C24

NACA RM No. L8C24

7129

[redacted]

Cy2

NACA

RESEARCH MEMORANDUM

FLIGHT TEST OF NACA FR-1-B, A LOW-ACCELERATION ROCKET-PROPELLED VEHICLE FOR TRANSONIC FLUTTER RESEARCH

By

Ellwyn E. Angle, Sherman A. Clevenson,
and Reginald R. Lundstrom

Langley Memorial Aeronautical Laboratory
Langley Field, Va.

NATIONAL ADVISORY COMMITTEE
FOR AERONAUTICS

WASHINGTON
July 20, 1948

[redacted]

319 98/13

Classification cancelled (or changed to UNCLASSIFIED)

By Authority of NASA Tech Pub Announcement #95
(OFFICER AUTHORIZED TO CHANGE)

By 10 Jan 53

(GRADE OF OFFICER MAKING CHANGE)

12 Apr 61
DATE

 [redacted]

NATIONAL ADVISORY COMMITTEE FOR AERONAUTICS

RESEARCH MEMORANDUM

FLIGHT TEST OF NACA FR-1-B, A LOW-ACCELERATION ROCKET-PROPELLED VEHICLE FOR TRANSONIC FLUTTER RESEARCH

By Ellwyn E. Angle, Sherman A. Clevenson, and Reginald R. Lundstrom

SUMMARY

A low-acceleration transonic flutter test vehicle was launched and flown by the Langley Pilotless Aircraft Research Division at its testing station at Wallops Island, Va. Flutter data were obtained on two similar sweptback wings (making use of radio telemetering) which indicated that wing flutter was symmetrical in mode. Flutter developed in both wings at approximately the same Mach number $(M = 0.65)$ and frequency (37 cycles per second). The left wing failed at $M = 0.705$, whereas the right wing remained on the model throughout the entire flight. The flutter speed determined from two-dimensional theory for an unswept wing in an incompressible flow is not conservative when compared to the experimental normal-flow flutter speed. A flutter-speed comparison of the NACA FR-1-B and FR-1-A models based on their wing-failure speeds appears to be meaningless. By installing strain-gage-type telemeters in the models, definite flutter frequencies and experimental flutter speeds may be obtained.

INTRODUCTION

In an effort to obtain information on wing flutter in the transonic range to assist in the wing design of high-speed airplanes, the NACA is investigating various means of conducting flutter tests in the transonic and supersonic speed ranges. These various techniques are described in references 1, 2, and 3. One technique involves the use of a low-acceleration rocket-propelled research vehicle to carry various test wings (of known flutter parameters) in transonic free flight. The results of the initial flight test of this vehicle, which has been designated the NACA FR-1, are reported in reference 1. This reference indicates that the flutter speed and flutter frequency should be obtained in addition to failure speed to give a more detailed picture of the flutter phenomenon in the transonic speed range.

[redacted]

The second in this series of flutter test vehicles equipped to measure flutter frequency as well as failure speed has been launched, and a successful flutter record was telemetered. The results of this flight are presented herein.

SYMBOLS

c	airfoil chord perpendicular to leading edge, inches
l	airfoil length along leading edge outboard of body, inches
E.A.	distance of elastic axis of wing behind leading edge, percent chord
C.G.	distance of center of gravity of wing behind leading edge, percent chord
a	nondimensional elastic-axis position $\left(\frac{2 \times \text{E.A.}}{100} - 1\right)$ (reference 4)
$a + x_\alpha$	nondimensional center-of-gravity position $\left(\frac{2 \times \text{C.G.}}{100} - 1\right)$ (reference 4)
M	Mach number
b	semichord in feet $\left(\frac{c}{2 \times 12}\right)$ (reference 4)
ρ	air density, slugs per cubic foot
$1/\kappa$	weight ratio $\left(\pi\rho b^2/m\right)$, where m is mass of airfoil per unit length (reference 4)
p_s	static pressure, pounds per square foot
T	free-air temperature, °F absolute
t	time after firing, seconds
q	dynamic pressure, pounds per square foot $\left(\frac{1}{2}\rho V^2\right)$
V	air velocity, feet per second
V_{f_e}	model velocity at start of wing flutter, miles per hour
h	geometric altitude, feet

GJ	torsional rigidity, pound-inches^2
f_{f_e}	experimental wing-flutter frequency, cycles per second
f_{h_1}	first bending natural frequency, cycles per second
f_{h_2}	second bending natural frequency, cycles per second
f_t	first torsion natural frequency, cycles per second
f_α	first torsion frequency (uncoupled) about elastic axis, cycles per second
f_{f_o}	reference wing-flutter frequency, cycles per second $\left(\text{analysis similar to that used in determining } V_{f_o}\right)$
V_{f_o}	reference wing-flutter velocity perpendicular to leading edge, miles per hour (based on theory for two-dimensional unswept wing in an incompressible medium employing first bending frequency and uncoupled torsion frequency and density of testing medium at time of beginning of flutter (reference 4))
V_{D_o}	reference wing-divergence speed, miles per hour (based on theory for two-dimensional unswept wing in an incompressible medium employing uncoupled torsion frequency and density of testing medium at time of beginning of flutter (reference 4))
$v/b\omega_\alpha$	nondimensional flutter-velocity coefficient where $\omega_\alpha = 2\pi f_\alpha$ (reference 4)

APPARATUS AND METHODS

Model

The NACA FR-1-B was a tailless airplane similar to the FR-1-A configuration. A sketch of the model is shown in figure 1, and its physical characteristics are listed in table I.

The flutter parameters obtained from static and vibration measurements made of the horizontal wings are listed in table II.

Instruments

Telemeter.- The telemeter consisted of two strain-gage channels (one for each flutter test wing) to record torsional flutter frequency by use of the strain variations on the surface of the wing during flutter and one inductance channel to record signals from a longitudinal accelerometer. A breakwire was routed through each wing and so connected into its strain-channel circuit that the breaking of the wire tuned the transmitter off that channel and resulted in "noise" or "hash" instead of a definite signal on the oscillograph record. This arrangement made it possible to determine the time of failure even if the wing failed outboard of the strain gages. Positions of the strain gages are shown in figure 1.

Radar and cameras.- The radar and camera installations were similar to those listed in reference 1, consisting of a continuous-wave Doppler radar and motion-picture cameras.

Radiosonde.- A radiosonde was released immediately after the flight to determine atmospheric conditions prevailing at that time. The results are shown in figure 2 as a plot of the velocity of sound and density of air against altitude.

Launching Technique

The launching rack, launching angle, and break-link assembly were identical with those used for launching the NACA FR-1-A and are described in reference 1.

Flight-Path Approximation

The initial part of the flight path was taken from the sequence of K-24 pictures shown in figure 3. The remainder of the flight path was calculated by a step-by-step method assuming infinite stability. The results of the calculations are shown in figure 4 as plots of altitude and horizontal distance against time.

RESULTS AND DISCUSSION

Flight

The launching of the NACA FR-1-B was performed successfully. One-half second after the model left the rack its attitude changed abruptly from 60° to 15° as can be seen in figure 3. This rapid change in attitude might be explained by two conditions that existed at the time of launching. First, wind gusts up to 17 miles per hour prevailed at that time and, second, the model possessed a large amount of static stability. The remainder of the flight, however, was smooth and at a very low altitude. At $t = 6.75$ seconds after firing, the left wing fluttered and failed. (See copy of telemeter record shown in fig. 5.) After wing failure, the flight path assumed a helical pattern and the model dived into the sea. Motion pictures confirmed visual observation that no roll was developed during the portion of the flight that the wings remained on the model.

The radar did not function properly; therefore, it was necessary to determine the velocity by integrating the accelerometer record (curve a, fig. 6), the results of which are shown as curve b, figure 6. A plot of Mach number against time is shown in figure 7.

Flutter

The time history of the flight of the NACA FR-1-B is shown in figures 4, 6, and 7 as the variation of altitude, horizontal distance, acceleration, velocity, and Mach number with time. Conditions at the time of the beginning of wing flutter are as listed in table III.

The telemeter record (fig. 5) shows that flutter occurs as a symmetrical mode and with a frequency of 37 cycles per second. The influence of the bending-frequency ratio f_h/f_α on the flutter-frequency ratio f/f_α, determined by use of the two-dimensional unswept theory (reference 4), is shown in figure 8. From this figure it is seen that, at the first-bending-frequency ratio of 0.263, the reference flutter-frequency ratio is 0.545 and yields a flutter frequency of 37.5 cycles per second.

The left wing fluttered at a Mach number of 0.657 and failed at a Mach number of 0.705. The right wing fluttered at a Mach number of 0.647, but motion pictures showed that it remained on the model throughout the entire flight, probably due to the destruction of the symmetry of the model after the failure of the left wing.

Figure 9 shows the influence of the bending-frequency ratio f_h/f_α on the flutter coefficient $v/b\omega_\alpha$ for an unswept thin airfoil of infinite aspect ratio in an incompressible flow. (See reference 4.) It is seen from this figure that the flutter-speed coefficient is 2.65 (first-bending-frequency ratio of 0.263), yielding the reference flutter speed V_{f_o} of 376 miles per hour $(M = 0.488)$. This analysis applies to the normal flow of a two-dimensional wing and cannot be applied directly to a swept wing.

For purposes of making an arbitrary comparison of the swept-wing flutter speed with the reference speed, the flow normal to the leading edge of the swept wing may be taken as a reference. Thus, the flutter started at a stream Mach number of 0.657 which corresponds to a normal-flow Mach number of 0.464. It may be noted that this experimental normal-flow flutter Mach number, although in closer agreement with the reference Mach number $(M = 0.488)$, is lower than the reference Mach number

(0.464 compared to 0.488). The reference Mach number is V_{f_o} divided by the speed of sound at time of wing flutter. As in the case of flutter bomb FB-4000 (reference 2, table II), the reference flutter speed is seen to be unconservative when compared to the component of the free-stream experimental flutter speed perpendicular to the leading edge.

Comparing the flight of the NACA FR-1-B with the FR-1-A, it is seen that both models lost one wing at different failure speeds. The failure speed of the FR-1-A was determined by breakwire installation. It may be noted that a swept wing may flutter for a considerable period of time before failure (reference 2, fig. 14). It is possible that two similarly constructed wings could have different failure speeds due to the variable length of time of flutter of wings while the rocket is still accelerating. Because of these reasons, a flutter-speed comparison of the wings on the two rocket models based on wing-failure speeds appears meaningless. Using strain-gage-type-telemeter installations in the rockets gives definite flutter frequencies and experimental flutter speeds.

CONCLUDING REMARKS

A technique has been developed using a low-acceleration rocket with telemeter for determining the quantitative flutter characteristics of wings in a free air stream.

The telemetered flutter record obtained during the flight of the FR-1-B showed the following:

1. The flutter was a symmetrical mode of flutter at 37 cycles per second.

2. One wing fluttered at a Mach number of 0.657 and failed at a Mach number of 0.705.

3. The other wing fluttered at a Mach number of 0.647 and remained on the model throughout the entire flight.

The experimental normal-flow flutter speed, although in closer agreement with the reference flutter speed than the measured flutter speed V_{f_e}, is lower than the reference flutter speed.

Since there is the possibility that two similarly constructed wings may have total failure at different speeds as well as the possibility of sustained flutter before failure, a flutter-speed comparison of the

NACA FR-1-B and FR-1-A rocket [redacted] wing-failure speeds appears meaningless. The use of strain-gage-type-telemeter installations in the rockets gives definite flutter frequencies and experimental flutter speeds.

Langley Memorial Aeronautical Laboratory
National Advisory Committee for Aeronautics
Langley Field, Va.

REFERENCES

1. Angle, Ellwyn, E.: Initial Flight Test of the NACA FR-1-A, A Low-Acceleration Rocket-Propelled Vehicle for Transonic Flutter Research. NACA RM No. L7J08, 1948.

2. Clevenson, S. A., and Lauten, William T., Jr.: Flutter Investigation in the Transonic Range of Six Airfoils Attached to Three Freely Falling Bodies. NACA RM No. L7K17, 1948.

3. Barmby, J. G., and Teitelbaum, J. M.: Initial Flight Tests of the NACA FR-2, A High-Velocity Rocket-Propelled Vehicle for Transonic Flutter Research. NACA RM No. L7J20, 1948.

4. Theodorsen, Theodore, and Garrick, I. E.: Mechanism of Flutter - A Theoretical and Experimental Investigation of the Flutter Problem. NACA Rep. No. 685, 1940.

[redacted]

TABLE I

PHYSICAL CHARACTERISTICS OF MODEL NACA FR-1-B

Weight, lb	252
Fuselage:	
Length, in.	93
Maximum diameter, in.	10.625
Horizontal wings:	
Weight (each), lb	6.00
Area (total), sq ft	7.45
Area (exposed), sq ft	6.18
Span, ft	5.25
Aspect ratio	3.7
Airfoil section (normal to leading edge)	NACA 65-009
Sweepback angle, deg	45
Loading, lb/sq ft	39.8
Mean aerodynamic chord, in.	17
Taper ratio	1:1
Critical Mach number	0.79
Vertical wings:	
Area (total), sq ft	3.40
Area (exposed), sq ft	2.22
Span, ft	2.55
Airfoil section (normal to leading edge)	NACA 65-009
Sweepback angle, deg	60
Loading, lb/sq ft	115
Mean aerodynamic chord, in.	16
Taper ratio	1:1
Critical Mach number	0.79

TABLE II

AIRFOIL FLUTTER PARAMETERS

	Left wing	Right wing
f_{h_1}	17.4	18
f_{h_2}	130	133
f_t	68.7	71.5
f_α	66.1	68.9
l	37.1	37.1
b	0.5	0.5
a	-0.24	-0.24
E.A.	38	38
$a + x_\alpha$	-0.12	-0.12
C.G.	44	44
$r_\alpha^{\ 2}$	0.21	0.21
$1/\kappa$ (standard)	26.1	26.7

NACA

[redacted]

TABLE III

INFORMATION AT TIME OF WING FLUTTER

Parameter	Left airfoil	Right airfoil
M	0.657	0.647
V_{f_e}	506	500
$V_{f_e} \cos 45^\circ$	358	354
ρ	0.00230	0.00230
q	295	287
p_s	2100	2100
T	532	532
t	6.36	6.28
h	225	230
$1/\kappa$	27	27.6
f_{f_e}	37	37
f_{f_o}	37.5	37.5
V_{f_o}	376	391
V_{D_o}	469	491
GJ	316,000	355,000

[redacted]

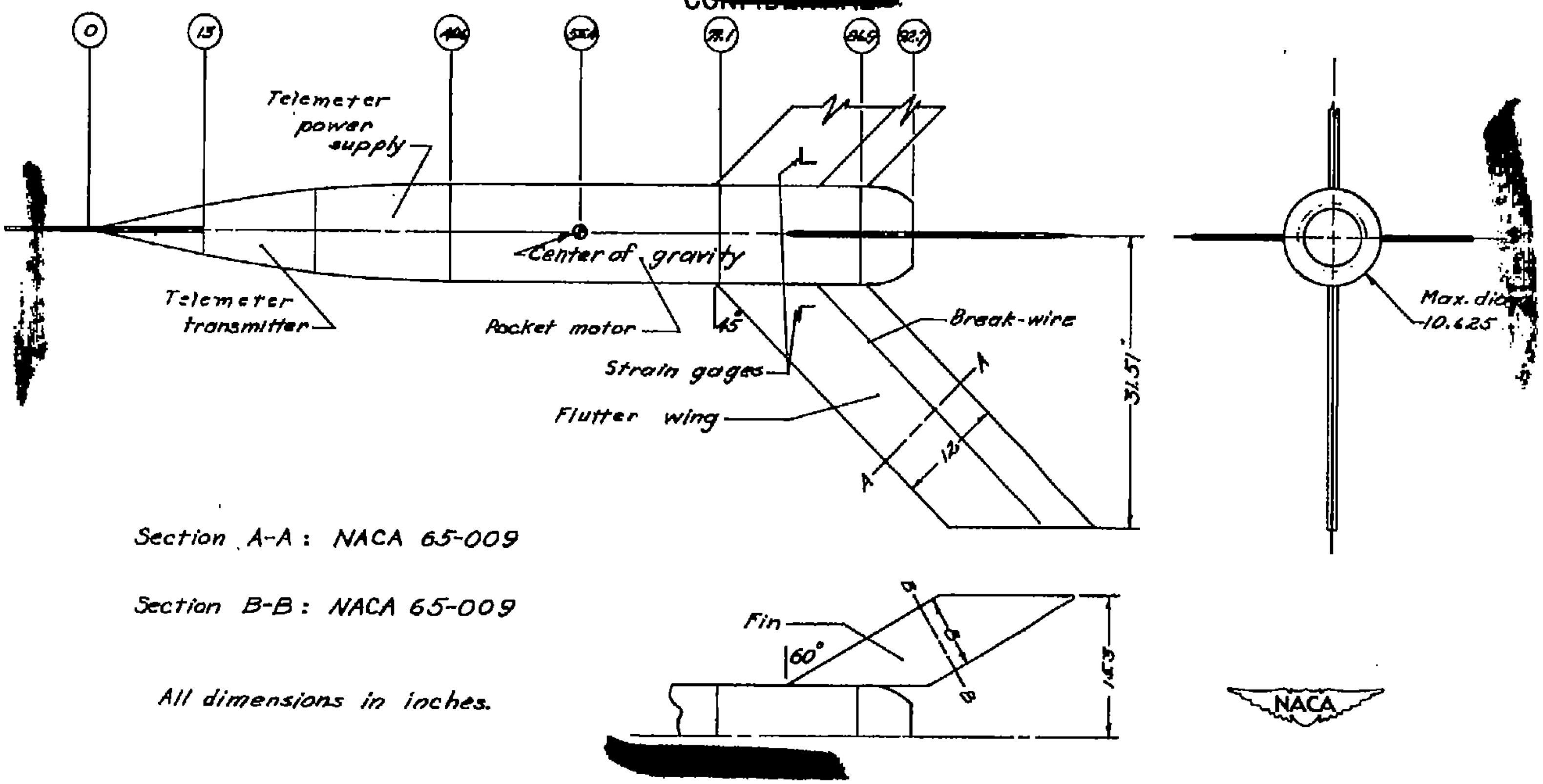

[redacted]

Figure 1.- FR-1-B flutter test rocket.

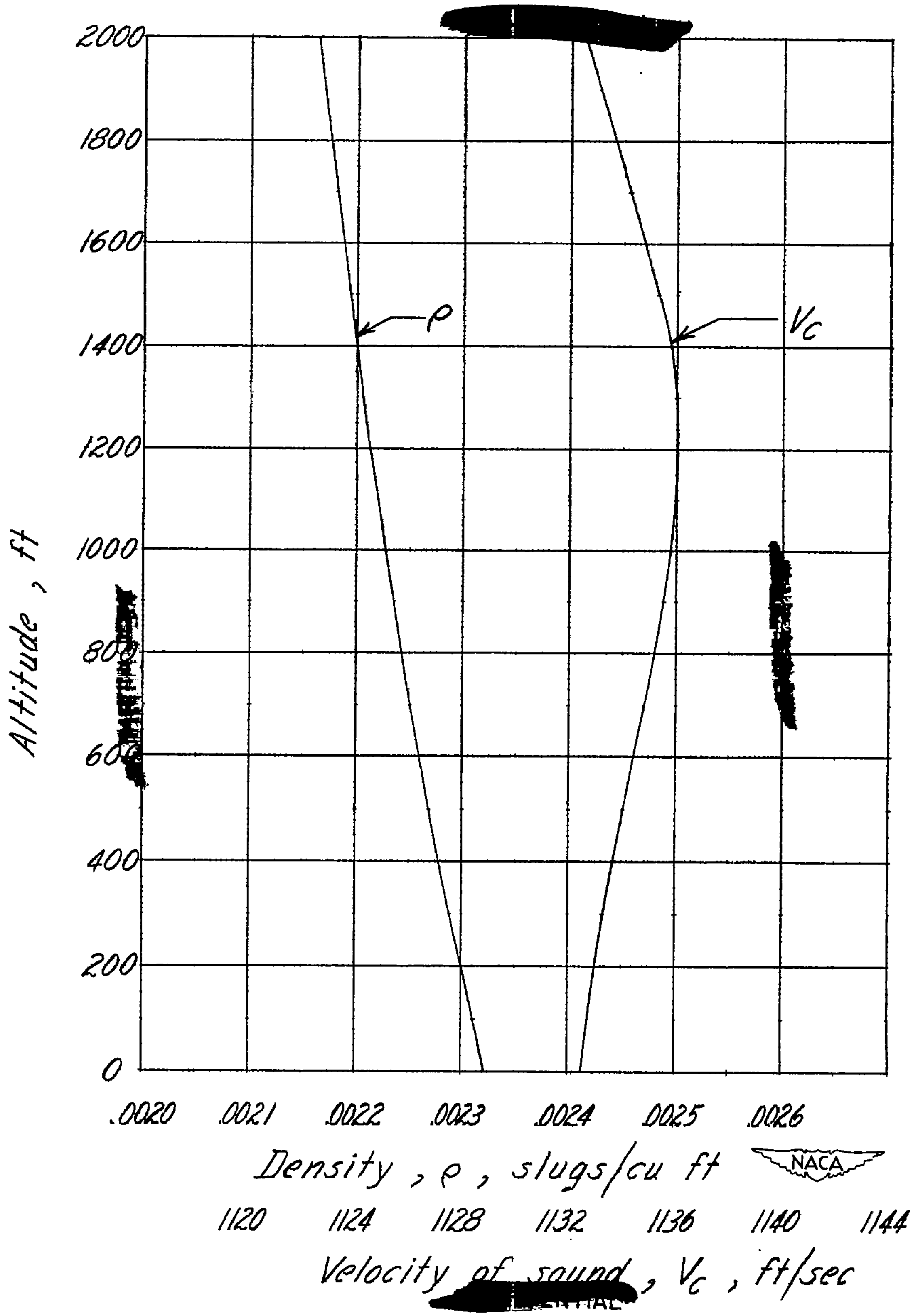

Figure 2.- Results of radiosonde record.

[redacted]

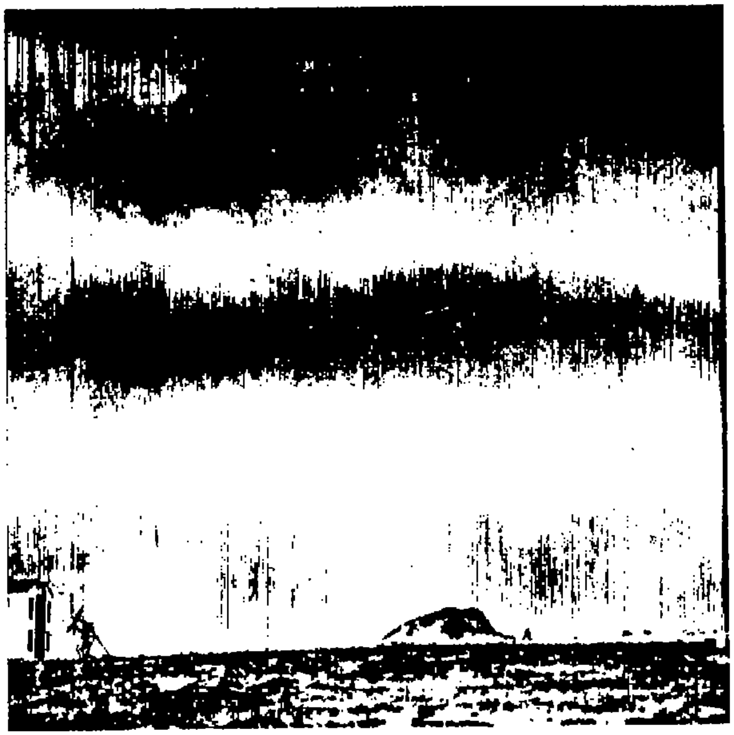

Time, 0 sec L-53642

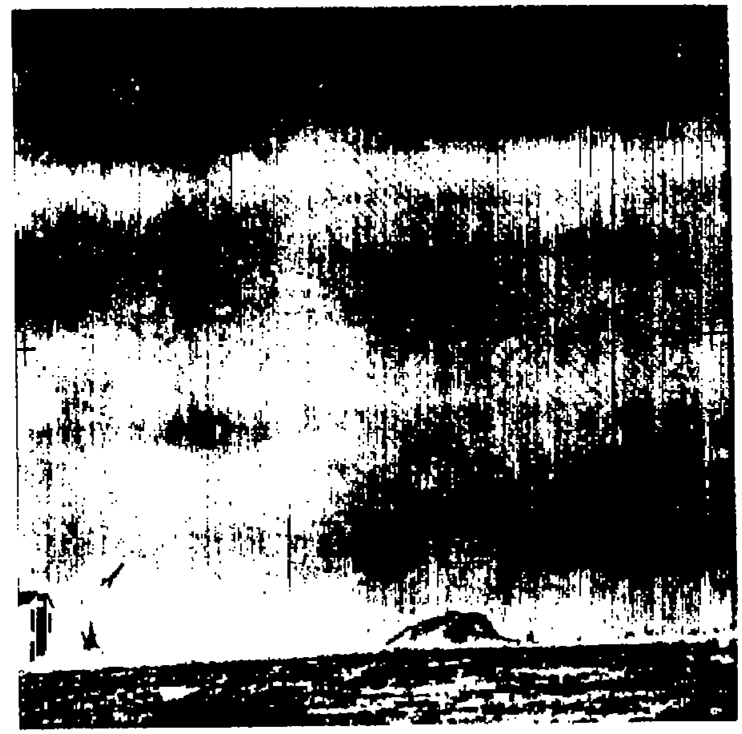

Time, 1.0 sec L-53644

Figure 3.- Sequence of pictures of the first 2.5 seconds of flight of the FR-1-B taken with K-24 camera.

[redacted]

[redacted]

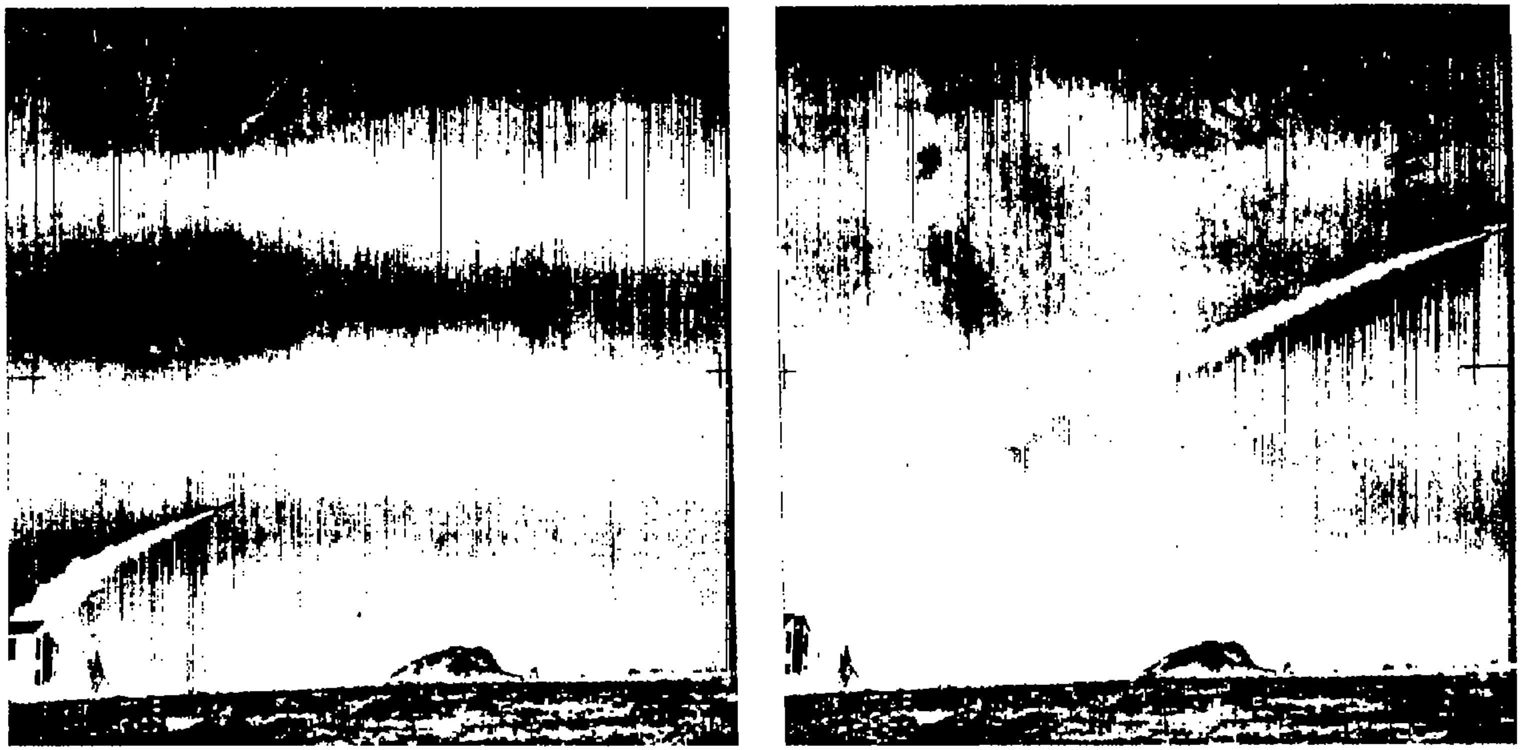

Time, 1.5 sec L-53645

Time, 2.5 sec L-53647

Figure 3.- Concluded.

[redacted]

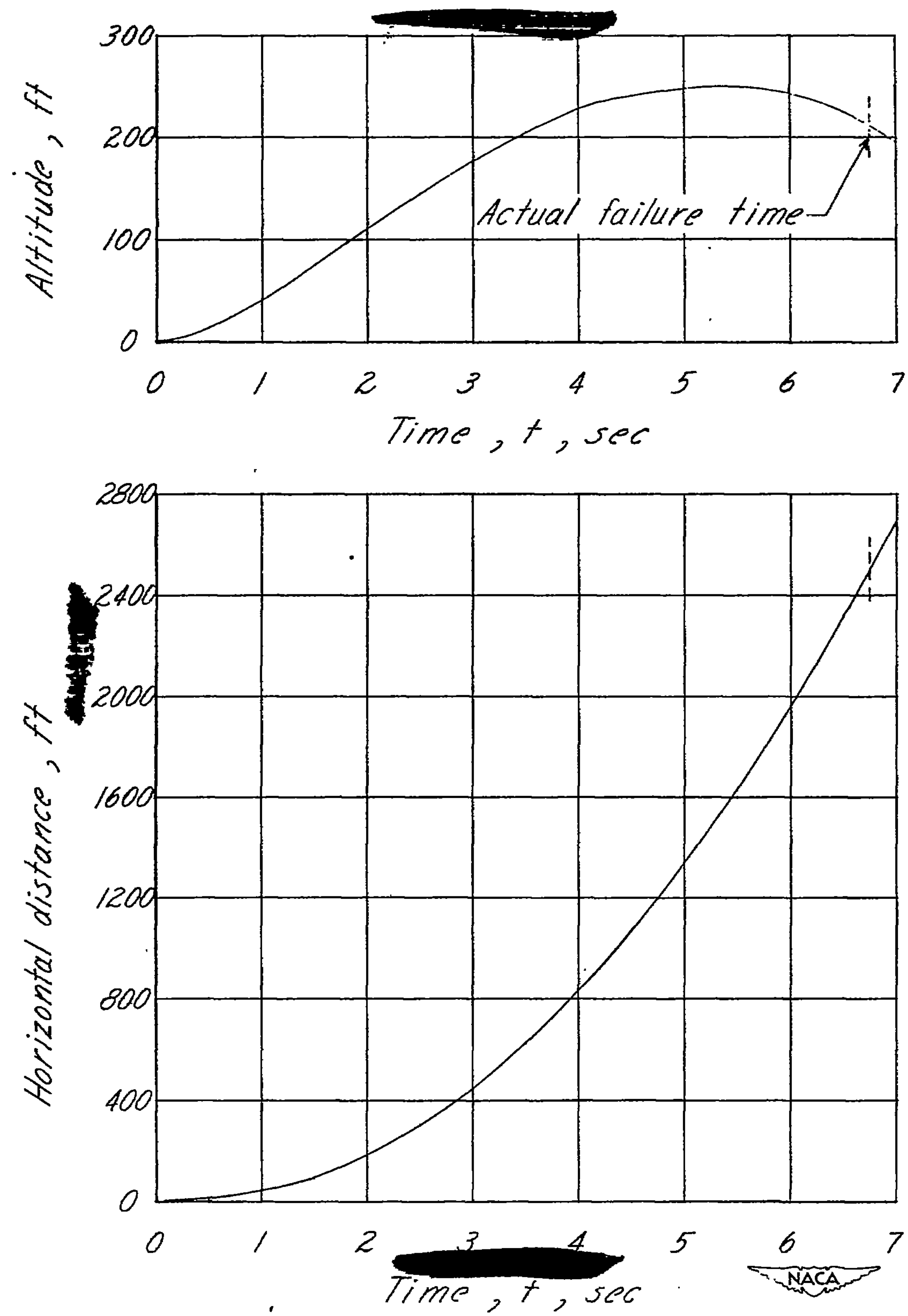

Figure 4.- Calculated trajectory characteristics of the FR-1-B.

[redacted]

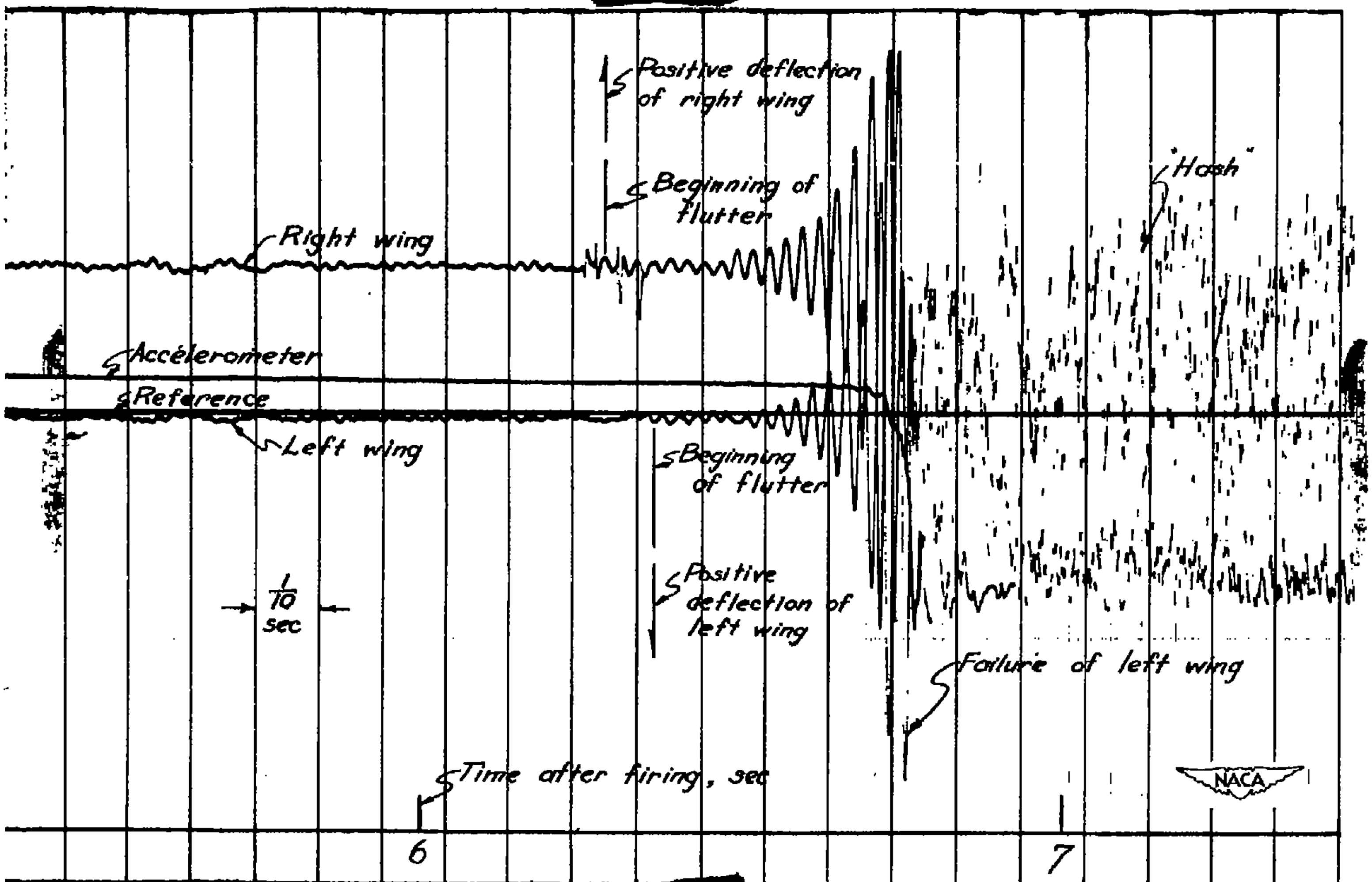

CO[redacted]

Figure 5.- Portion of telemetered record showing wing flutter.

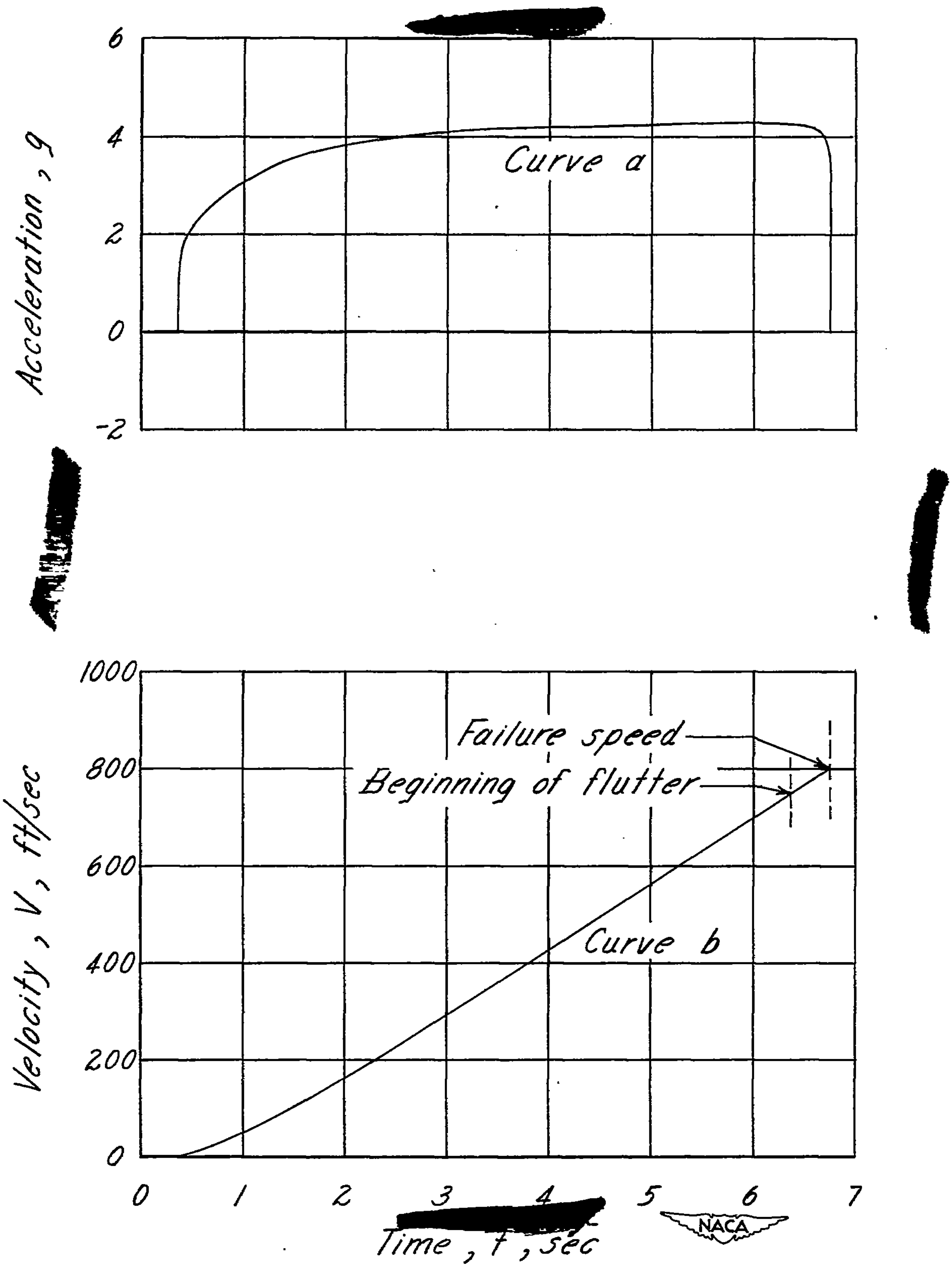

Figure 6.- Variation of acceleration and velocity against time.

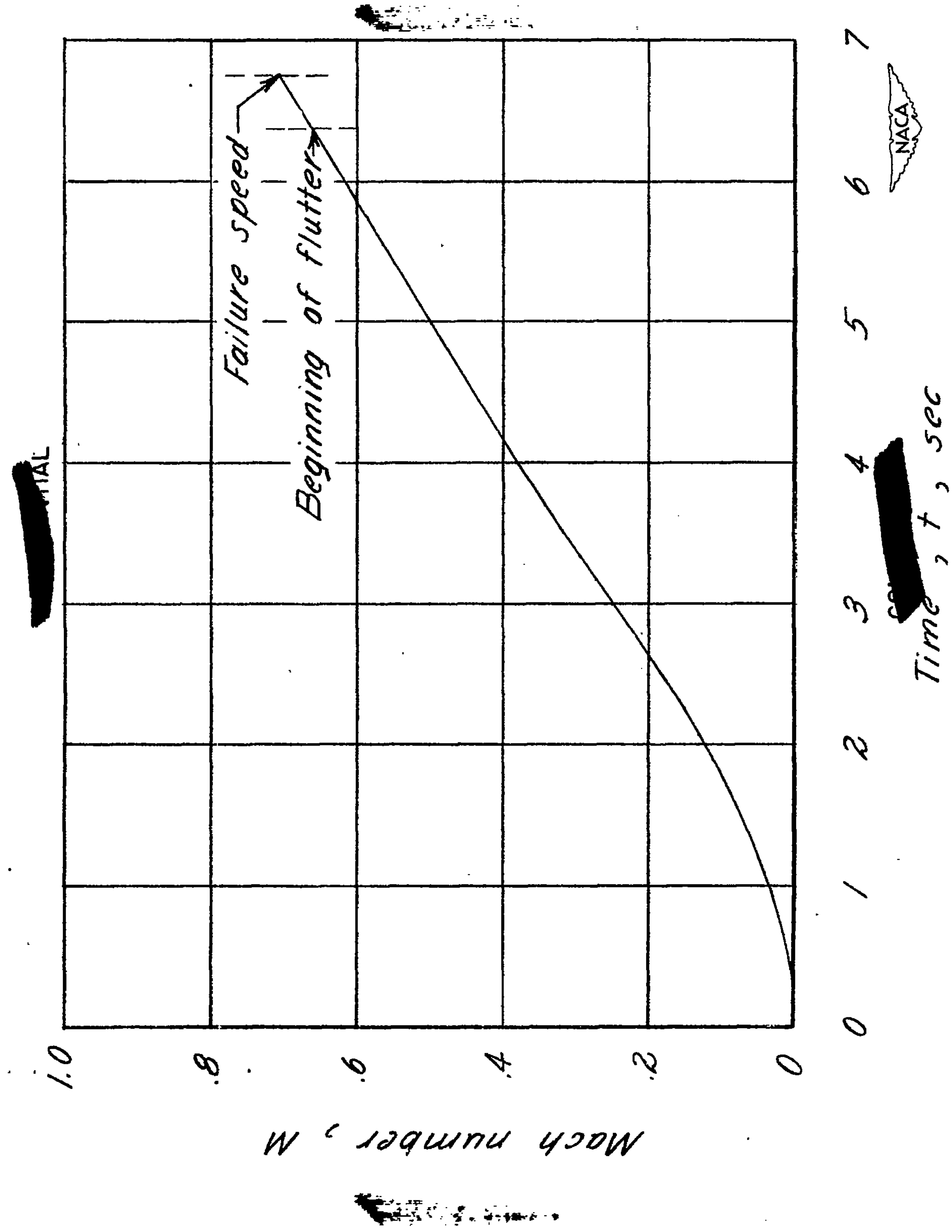
Failure speed
Beginning of flutter
Mach number, M
Time, t, sec
NACA
0
.2
.4
.6
.8
1.0
0
1
2
3
4
5
6
7

[redacted]

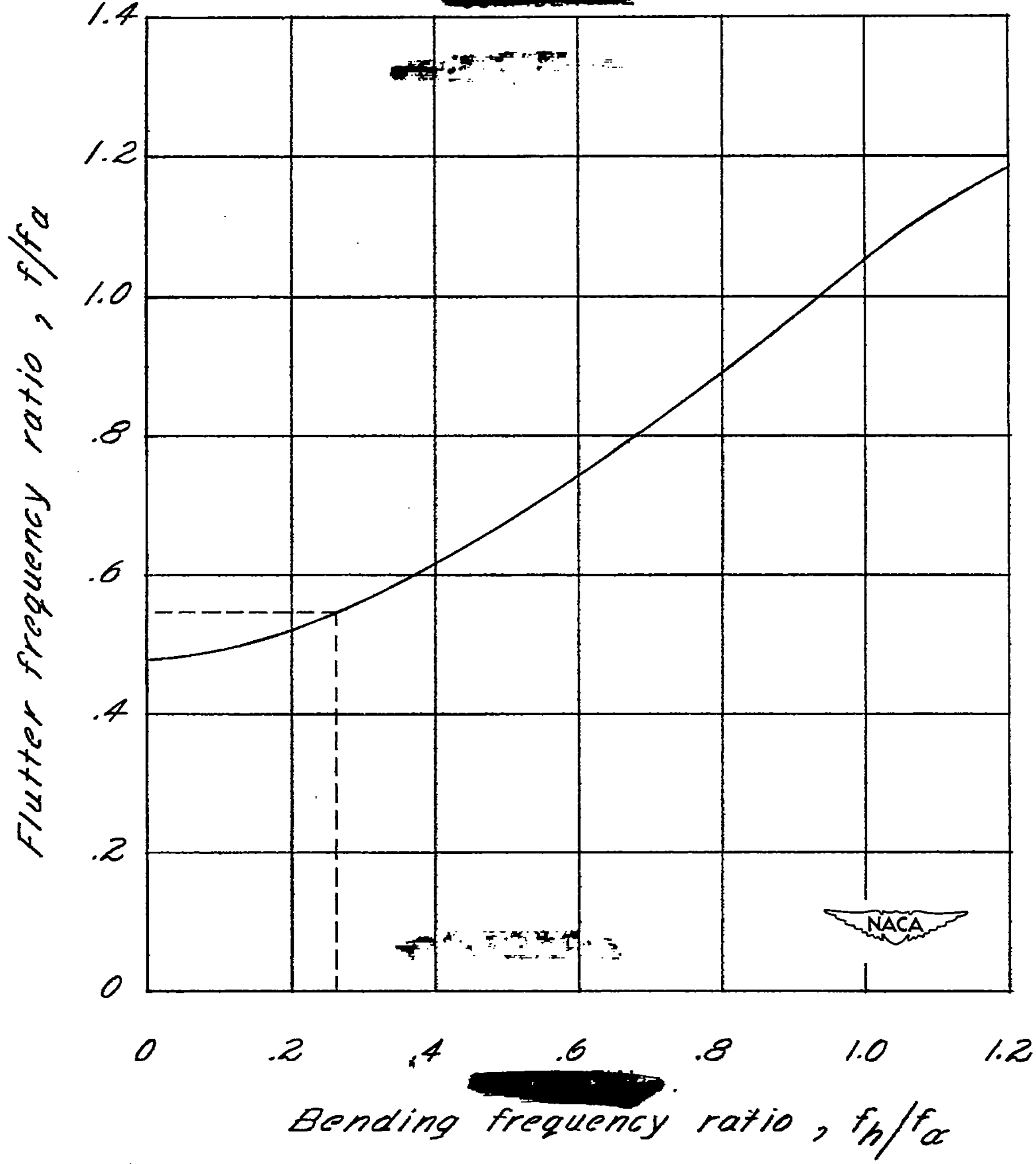

[redacted]

Figure 8.- Variation of flutter frequency ratio against bending frequency ratio.

[redacted]

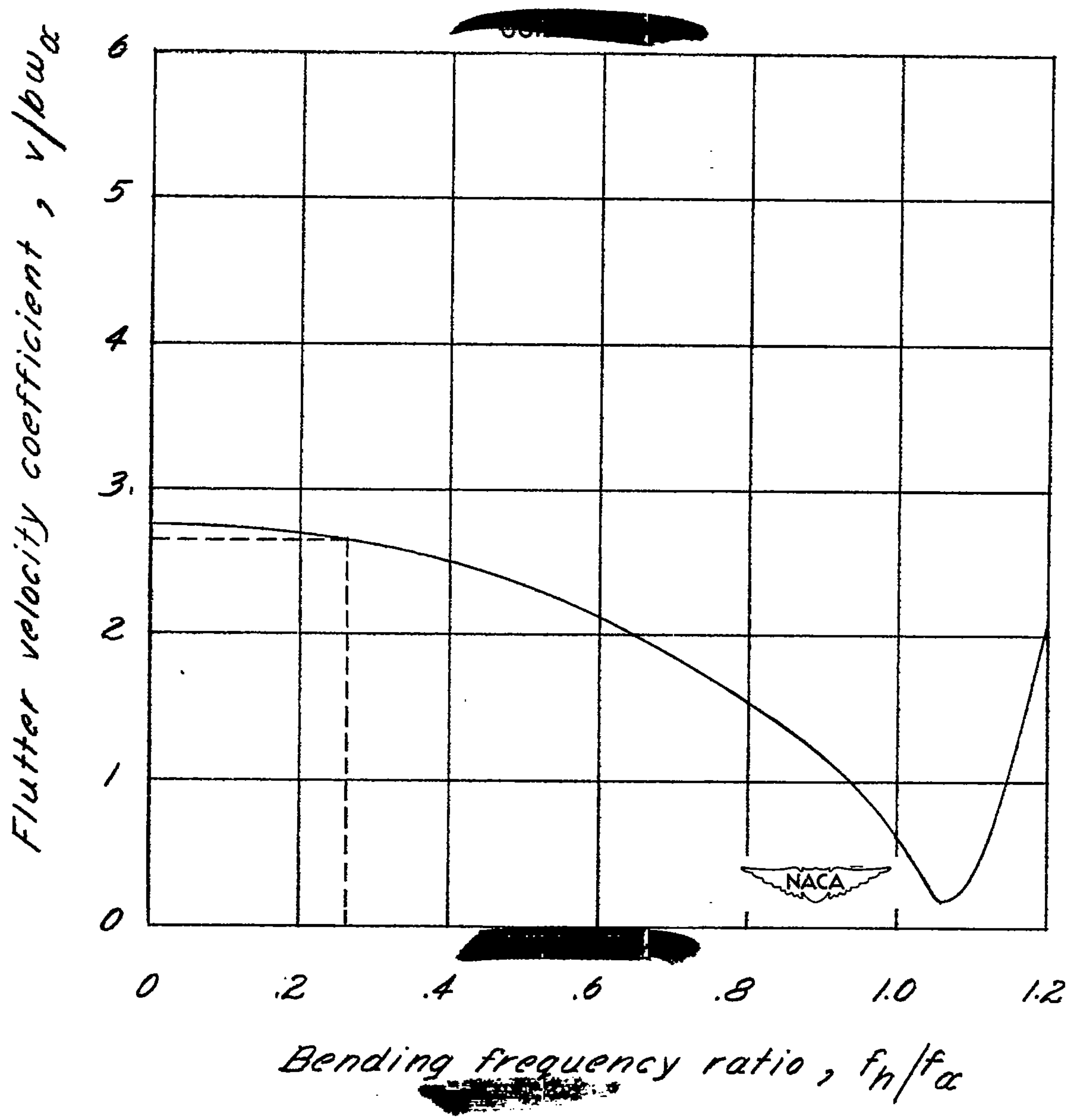

Figure 9.- Variation of flutter velocity coefficient against bending frequency ratio.